FINITE ELEMENT IMPACT MODELLING OF SHOT PEEN FORMING

Evandro Cardozo da Silva, evandro.cardozo@joinville.ufsc.br
UFSC – Universidade Federal de Santa Catarina - CEM - Mobility Engineering Center
R. Paulo Malschitzki nº 10 – Campus Universitário – Zona Industrial
CEP: 89219-710

Sérgio Tonini Button, sergio1@fem.unicamp.br
DEMa- Department of Materials Engineering – UNICAMP
UNICAMP, DEMa-FEM-UNICAMP, Caixa Postal 6122, Campinas – SP/CEP 13.083-970

Renato Pavanello, pava@fem.unicamp.br
DMC- Department of Computational Mechanics – UNICAMP
UNICAMP, DMC-FEM-UNICAMP, Caixa Postal 6122, Campinas – SP/ CEP 13.083-970

Abstract: *Manufacturing of complex and large components of airplanes is only possible by modern techniques like the well-known shot peen forming. The improvement of that forming process comes from simulation with commercial Finite Element Method (FEM) softwares like Marc, Dytran, Ansys, ABAQUS and others. The optimization of tridimensional dynamic method that represents virtually the process is based on the validation of the numerical experiment by reproducing processing parameters defined by some studies found in the literature. Impact modelling and peen forming simulation, using MSC.Dytran, are explored in this work to contribute to the understanding of this important manufacturing process. It is shown that is possible to calculate the profile of residual stresses and the final shape of the piece.*

Keywords: *Shot Peening, Residual Stress, Numerical Simulation, Aluminum Alloy.*

1. INTRODUCTION

Shot peening (SP) is a cold working process widely used to increase the fatigue strength and surface hardness, as consequence of developing compression residual stresses and strain hardening, respectively. The controlled distortion of shot peened sheets is the basis of peen forming (PF) which is ideal to form shapes of large metallic panels. Nowadays many researches have been presented to develop a method to form more complex and large components for some specific areas like aerospace, airplane and cars industry.

The greatest challenge of this work is to determine an appropriate model to simulate PF considering accuracy and efficiency. One of the limitations of simulation by FEM is the available computational resources to direct simulate the real process, circumvented by applying equivalent loads (Silva *et al.*, 2006). The simulation accuracy lies in studying the phenomenon locally and extending the results to the rest of the workpiece to achieve a model which best represent the forming process.

2. FINITE ELEMENT MODELING

2.1. Dynamic Three-dimensional Finite Element (FE) Modeling of SP

Models from simple impact to multiple dispersed impacts are considered using the commercial finite element (FE) code of MSC (Patran/Implicit and Dytran/Explicit) (MSC, 2005).

The procedures of the process simulation had as main references the studies of Meguid *et al.* (1999a , 1999b e 2002) and Han *et al.* (2000a, 2000b e 2002).

2.1.1. Model of Simple Impact

Finite Element Model

In this work the dynamic elastic-plastic analysis of simple and double impacts was done with a FE explicit dynamic model using the MSC.Dytran commercial FE code. Figure 1 shows one quarter of the part geometry (workpiece) and one eighth of a sphere of radius *R* (small round steel shot), due to symmetry and to reduce the computational time. The dimensions of the part in the form of a block are 8 x 8 x 4 mm^3 (Han *et al.*, 2002) (Fig.1(a)). The dimensions defined by Meguid *et al.* (1999b) to evaluate the effect of the contours are also given to one quarter of the geometry with $W = 7R$ (length), $H = 4R$ (height) and $B = 5R$ (width) (Fig. 1(b)). The impact area is considered depending on the size of the shot.

A shot shell model was used, representing a significant computational time reduction of about eight times if compared to the solid element. In this model a steel rigid sphere (density ρ = 7850 kg/m^3) was defined for having much higher hardness than the component and for being more appropriate for most impact simulations (Meguid *et al.*, 2002). The mass of the shot serves as an input parameter of the FE code for simulation (R = 1.0 mm, and mass m = 4.11x10^{-6} kg). Table 1 shows the material constitutive model chosen as elasto-plastic for the block and rigid for the shot. The properties and their values are shown in Tab. 2 as input parameters of the FE code for simulation.

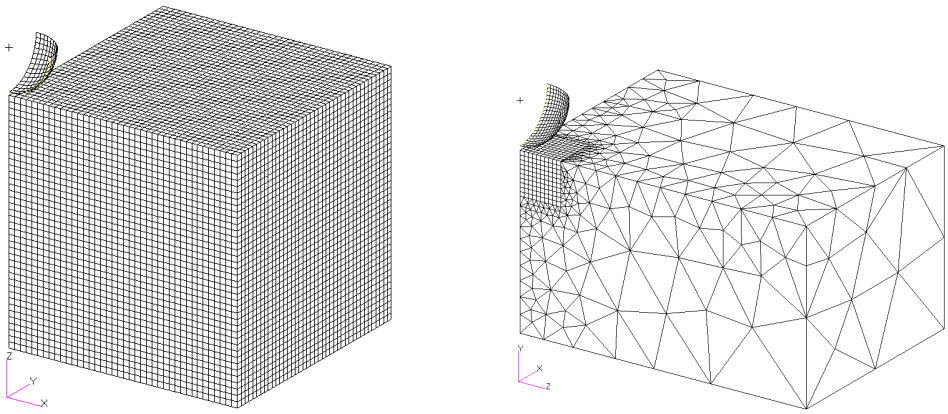

(a) (b)

Figure 1. The geometry and model discretization: (a) based HAN *et al.* (2002) and (b) based MEGUID *et al.* (1999b).

Table 1. Selection of material constitutive model of the block and the shot.

Input Parameters	**Block**	**Shot**
Constitutive Model	ElasPlas (DYMAT24)	Rigid (MATRIG)
Element Type	Lagrangian Solid	Shell
Yield Model	Bilinear	-
Strain Rate Model	Cowper Symonds	-
Failure Model	Maximum Plastic Deformation	-
Properties of Rigid Body	-	Geometric

Table 2. Material properties of the block and the shot.

Block Properties	**Steel**	**Al Alloy 7050 T7651**
Density (ρ) =	7.8x10^{-6} kg/mm^3	2.83x10^{-6} kg/mm^3
Elastic Modulus (E) =	200.0x10^3 MPa	72.0x10^3 MPa
Poisson Ratio (ν) =	0.3	0.33
Yield Stress (σ_y) =	600.0 MPa	450.0 MPa
Tangent Modulus (E_t) =	800.0 MPa	120.0 MPa
Sphere Properties	**Steel**	**Steel**
Density (ρ) =	7.85x10^{-6} kg/mm^3	7.85x10^{-6} kg/mm^3
Diameter (D) =	1.0	1.4
Mass (m) =	4.11x10^{-6}kg	1.12x10^{-5}kg

To discretize the target block, solid FE are used with eight-nodes (hexahedron - CHEXA) and four-nodes tetrahedron (CTETRA), both with high capacity of deformation and displacement. The first element was defined in the impact region due to its greater accuracy, and the second, for the rest of the piece (Meguid *et al.*, 2002). Several numerical experiments were done to test the numerical convergence (Silva, 2008), generating more than 100GB of data with various discretized geometries (Fig. 1) and discretized symmetry cell (Fig. 2(a)).

A symmetry cell model is the alternative that currently is adopted for simulation of SP for multiple impacts. The convergence tests were performed using many meshes for the geometry defined by HAN *et al.* (2002). HAN *et al.* (2000) considered that the size of the block element must be less than *D/10*, where *D* is the diameter of the shot. In this model, we opted initially to discretize the region of impact 2.1 x 2.1 x 4.0 mm^3 (number of elements: 30x30x20; element dimension: 0.07x0.07x0.08 mm^3; elements: 18000 CHEXA and 16482 CTETRA), adopting the symmetry cell

defined by refined *D*/20 mesh block (Fig. 2(a)). Figure 2(b) shows the component *XX* residual stress profile converged for a shot (1/8) mesh of 560 elements.

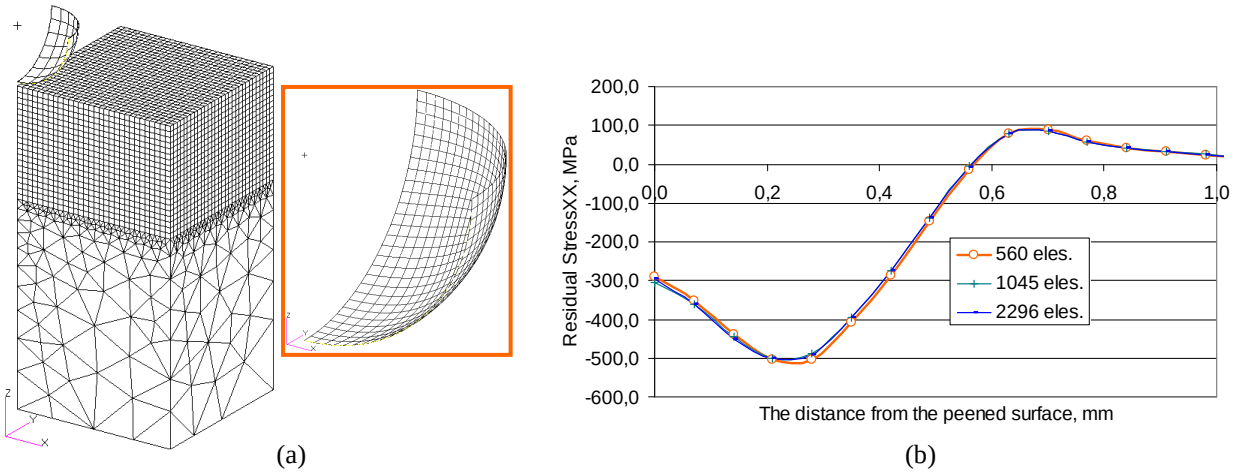

(a) (b)

Figure 2. Convergence of the residual stress profile of the sphere mesh and the symmetry cell with 2.1x2.1x4.0 mm^3 (v = 36.0 m/s): (a) meshes of block and shot and (b) stress profile

Oblique Impact Model

To verify the effect of an oblique simple impact a model was used with half-symmetry of the piece and different incidence angles ranging from 30^o to 90^o in respect to the normal direction to the incidence plane. The effect of friction coefficient μ was simulated for an incident angle of 30^o and varied from 0.0 a 0.5.

Strain Rate Effect

The main difficulty to solve the SP FE simulation is to obtain data of the sheet material and choose the most appropriate model for it. In SP it is common to establish only the hardness of the workpiece and of the shot. In general, there are no data of the stress-strain curve of the sheet material in the plastic region. Another major problem is the high strain rate involved in SP that reaches 6 x 10^5 s^{-1} (Meguid *et al*., 2002) for a time of impact about 2 μs.

The Cowper-Symonds power law, already implemented in MSC.Dytran was used to consider the strain rate:

$$\dot{\varepsilon}^{pl} = C\left(\frac{\sigma_{esc}}{\sigma_{din}} - 1\right)^{p}$$

where $\dot{\varepsilon}^{pl}$ is the rate of deformation, σ_{din} dynamic tension, σ_{esc} is the static yield stress, and C and p are constants of the material. The coefficients proposed by Majzoobi *et al.* (2005) were applied to validate the numerical simulations (LS-DYNA), adopting C = 2 x 10^5, p = 3.3 and σ_{esc} = 1500 MPa.

Implicit/Explicit Models, Materials, and Contact Damping

The FE implicit method has numerical difficulties even in quasi-static nonlinear problems due to the iterative approach used to achieve the convergence for highly nonlinear materials. The FE explicit method equations available in the software can be solved directly to determine the solution without iteration which and represent a more robust alternative method. The FE implicit method, more traditional, presents a smaller time solution for simple loading conditions, but for some loading conditions, like in dynamic contact, the explicit solution is advantageous.

To model the interface sphere/target ("master/slave" contact pair), contact elements were used for both bodies in which the FE explicit method is the best choice. The contact nodes were created in the surface of the block to be peened near the impact region and the bottom half of the sphere, since only these regions could be in contact. The friction coefficient μ = 0.25 used by Meguid *et al.* (1999a) and μ = 0.1, by Al-Hassani (1999) are some of the values found in the literature. Han *et al*. (2002) state that values greater than 0.2 have no significant influence on the profile of residual stress, as confirmed by Silva (2008).

2.1.2. Double Impact

A dynamic three-dimensional double impact model with two spheres placed side by side was developed to evaluate the effect of the proximity of the impacts on the profile of residual stress, as found in the work of Meguid *et al.* (1999b).

Silva (2008) describes the layout of the points of impact by two spheres of radius *R* distant by *d* and the discretized geometry of the components for the symmetry of the model with the same elements previously seen for the single impact. Strain rate sensitivity of the material is not considered, the coefficient of friction is $\mu = 0.2$, the sheet material is defined by Han *et al.* (2002), Table 2, and the impact velocity is 36.0 m/s.

2.1.3. Multiple Impacts

Dynamic modeling of multiple impacts is defined in this work by the dynamic elasto-plastic analysis of multiple local and distributed impacts with an algorithm for dynamic explicit finite element method. Local residual stress and strain profiles are obtained to be applied throughout the part as input data for the implicit static solution.

Finite Element Models

The first model considers the multiple concentrated impacts (punctual) and the second, the impact of multiple dispersed spheres of radius *R* which collide in a normal angle of incidence as shown in Fig. 3a and Fig. 3b.

The block dimensions are 2.1 x 2.1 x 4 mm^3 (3*R* x 3*R* x *H*). *H* corresponds to the thickness of the blasted plate and is kept to minimize the boundary conditions. The same sphere of the simple impact model was adopted and the properties of the aluminum block are provided in Table 2.

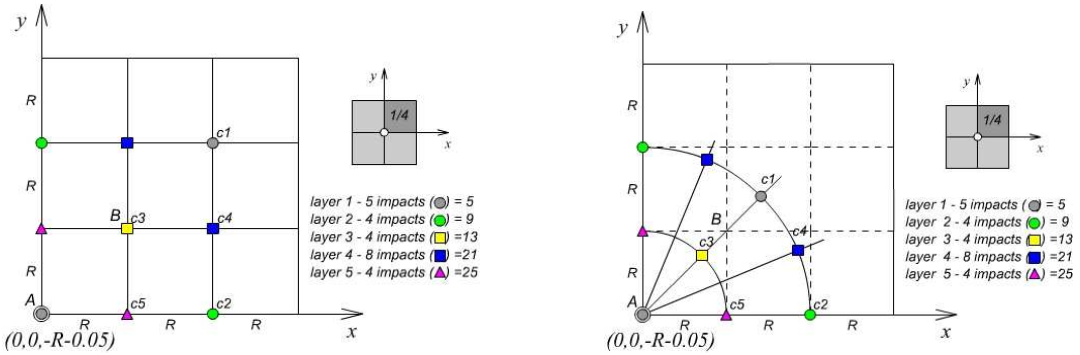

Figure 3. Scheme of the position of the points of dispersed impact: (a) cartesian and (b) radial.

The distance between the impacts is the radius R to assure enough time for the oscillations, caused by the current impact, not disturb the solution of the next impact. For a velocity $v = 36$ m/s the time between impacts is about 20 μs. The damping effect on the deformation at the impact point is calculated according to Silva (2008).

Levers and Prior (1998) observed that the explicit dynamic FEM to model the multiple impact is considered attractive in its efficiency and application in the process of PF. However, they found that the explicit method is truly dynamic so that the model can not reach the static equilibrium state simply extending the computational time. Therefore, adopting some parameters of damping, as adopted by Meguid *et al.* (2002), is an alternative to unwanted numerical oscillations associated with the explicit solution to this problem as considered by Silva (2008).

2.2 Static Three-dimensional FE Modeling of PF

After the explicit modeling of the SP multiple impacts, the profiles of stress and strain were obtained and applied in models for implicit static analysis, as an initial loading condition. The implicit method was used to solve the static problem and obtain the equilibrium with the final terms of plastic deflection and residual stress state. This procedure is justified because one can consider that stresses and strains are uniformly distributed in the horizontal direction and are the same for the same distance from the blasted surface. Therefore, the states of stress and strain are a function only of the coordinate in the thickness. Based on this hypotheses also mentioned by Han *et al.* (2002), one can use a coarse FE mesh in the horizontal direction reducing the model and obtaining a realistic PF solution.

In this work the solution is done using a shell element that most closely resembles the geometry of the parts that are peen formed. (Silva *et al.*, 2006) presents a model with composite shell element to simulate a plastic layer in the region near the blasted surface, whose thickness could be associated with the results obtained in the explicit model of SP multiple impacts. This layer corresponds to an elastic-plastic material and the rest of the plate thickness is assumed to be the elastic element model with the composite material. The explicit dynamic model mesh with solid element is transported to the implicit static model with the same distribution in the thickness of the plate.

3. RESULTS AND DISCUSSIONS

3.1. Dynamic Modelling of Shot Peening

3.1.1. Model Validation

Figure 4a shows the variation of speed throughout the shot impact against the surface of a steel workpiece modeled by MS.Dytran explicit code and compared with Meguid *et al.* (1999) (Tab.3) that used ANSYS implicit code. Czekanski and Meguid (2006) compare their FE model with the results of this example using the commercial explicit code LS-DYNA. They kept the initial shot velocity, used a strain hardening H =1000 MPa and the final shot velocity was 17.3m/s. Table 3 shows the results of these works. It was verified by Silva (2008) that increasing strain hardening of the surface from H = 800 to 1000 MPa, residual stress decrease by about 10%, and resulted in a final velocity of 15.6 m/s very close with the results of this work which did not use damping numerical values.

Table 3. Results of velocity variation during the entire impact process.

Parameters	Current Model	MEGUID *et al.*, 1999	Czekanski and Meguid (2006)
Initial shot velocity (m/s)	75	75	75
Strain Hardening (MPa)	800	800	1000
Contact time (μs)	1.75	1.7	1.7
Shot rebound start (μs)	1.3	1.25	1.25
Final shot velocity (m/s)	15.9	14.3	17.3
Coeficient of restitution (%)	21.2	19.1	23.1

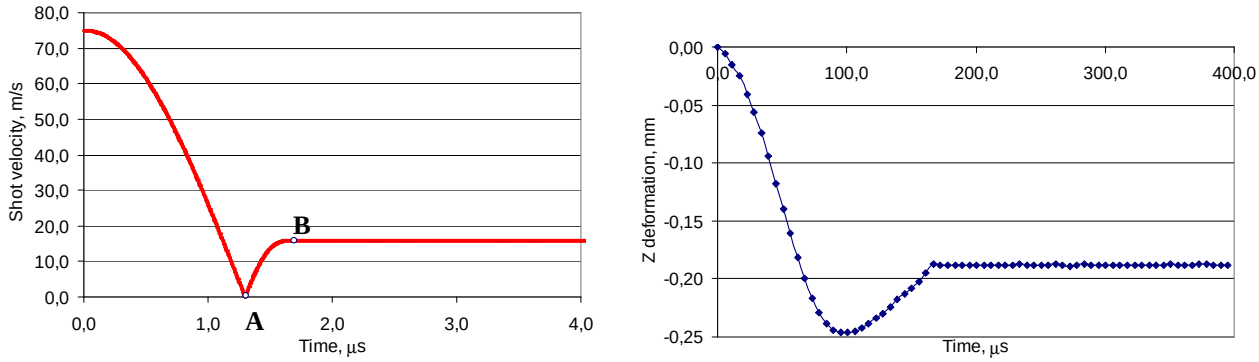

(a) (b)

Figure 4. Simple shot impact: (a) the time history of the velocity of the shot and (b) Z deformation history of the block at the impact point of the shot. (μ = 0.2; v = 6.3 m/s; R = 25mm)

Figure 4b shows the indentation using parameters of Kobayashi *et al.* (1998) for the dynamic impact test of a single steel shot against a flat plate of steel. The depth of indentation was 180 μm, while in the simulation with MSC.Dytran a depth of 187 μm was observed. Thus this simulation represents a good approximation compared to the dynamic test.

3.1.2. Single Impact

A finite element analysis of a single impact was done for an aluminum alloy Al 7050 T7651 sample with properties shown in Tab. 2, and considering the bilinear elastic-plastic behavior of the material. It was also considered a rigid steel sphere of radius R = 0.7 mm and a velocity of v = 36.0 m/s with density ρ = 7850.0 kg/m^3. Friction is not considered in that analysis.

The results are represented as graphs of the stress and deformation versus depth by selecting nodes on the centerline of the impact along the thickness, to determine the effect of different parameters (Silva, 2008), such as: velocity and size of the sphere, friction, strain hardening and strain rate and the effect of oblique impact with and without friction.

The effect of the sphere velocity was observed with 36, 72 and 108 m/s shown in Fig. 5 with the residual stress profile in *XX*. With increasing ball speed causes an increase in the compressive layer. From a certain velocity the Bielajev point also increases and moves into the sheet and the deformation increases proportionately (Silva, 2008).

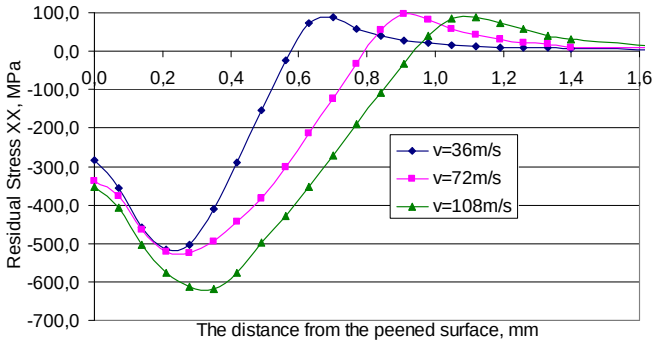

Figure 5. Residual stress profile in XX for three different shot velocity for a sphere radius R = 0.7 mm.

3.1.3. Double Impact

The stress profile at the point of impact decreases as the ball approached with a difference of about 10% for the Bielajev point, as shown in Fig. 6 for d/R = 1 e d/R = 2. For d/R < 1 there is uniformity in the residual stress profile to a value intermediate to the above ratios, and an increase in the depth of the plastic zone. This last condition is not physically possible for the simultaneous normal impact. However, in practice most of impacts are oblique to the plate and the duration of impact is extremely short (<2 μs, Fig. 4). Figure 7 shows the distribution for ratios d/R = 2, d/R = 1 and d/R = 0.4.

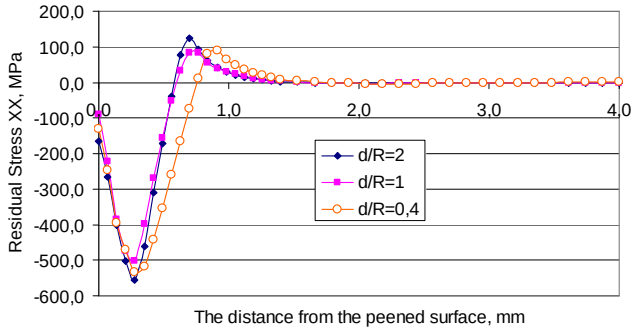

Figure 6. Residual stress profile on the center line of the block for three different ratios (d/R). (μ=0.2; α = 0.007).

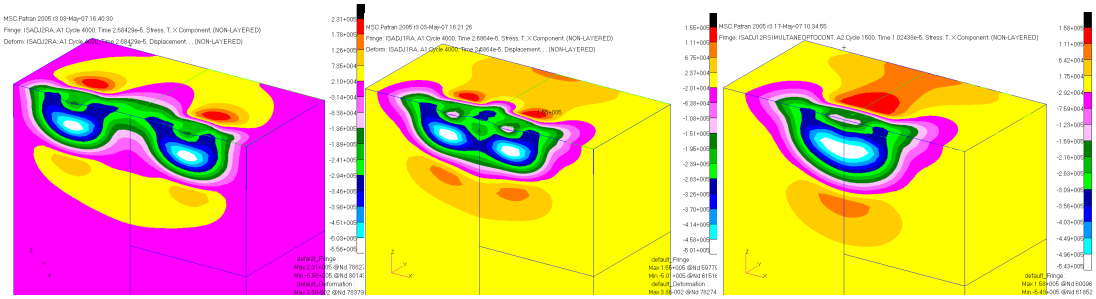

d/R = 2 d/R = 1 d/R=0,4

Figure 7. Residual stress distribution in XX (x10^{-3} MPa) for three different ratios (μ=0.2; α = 0.007).

3.1.4. Multiple Impact

The results are separated into a model that considers the multiple concentrated impacts and a model that most closely approximates the actual process that occurs in multiple impacts of dispersed balls against the sample. The last model may have various configurations in terms of distribution, here considered regularly distributed in the cartesian and radial coordinate systems (Fig. 3).

Multiple Concentrated Impacts

The model of multiple concentrated impacts simulated nine impacts against a sample with an arrangement of spheres that collide successively and resulted that saturation is established from 8 impacts as shown in Fig. 8 for the deformation in Z. There is a gradual convergence of deformation and stress results by increasing the number of impacts.

Figure 9 shows the results of MSC.Dytran of strain and tension distribution after nine impacts.

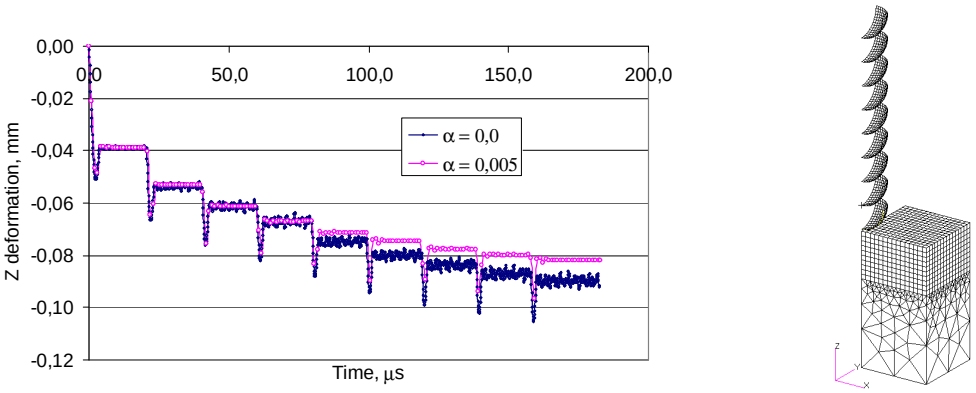

Figure 8. Convergence of deformation at the point of impact to multiple concentrated impacts model (α = damping).

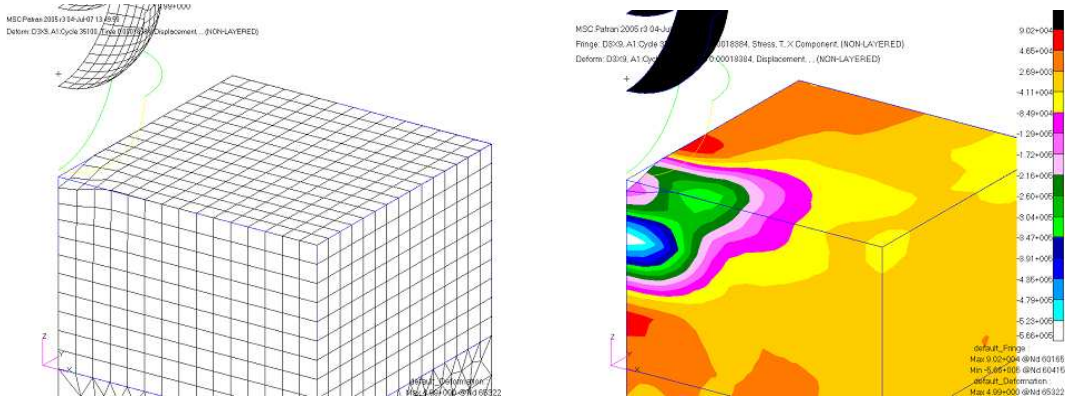

(a) (b)

Figure 9. Multiple concentrated impacts (9 spheres): (a) deformation, (b) tension - component *X*.

Multiple Dispersed Impacts

The numerical simulation of multiple impacts on an aluminum plate is developed using layers with 5, 9, 13, 21 and 25 impacts. The simulation in MSC.Dytran, adopts two types of regular distribution, called a Cartesian (50% coverage) and a radial (70% coverage) as shown in Fig. 3a and Fig. 3b, respectively.

- ***Cartesian Distribution***

Figure 10 shows the results of MSC.Dytran of strain and stress distribution after 25 impacts.

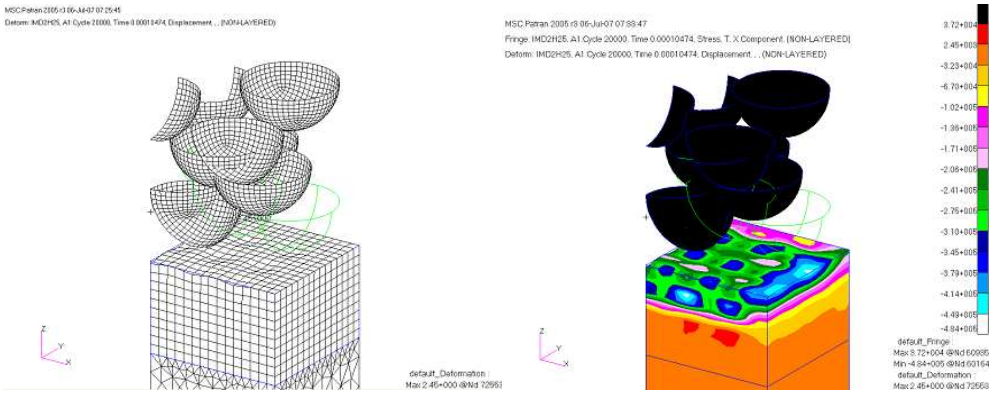

(a) (b)

Figure 10. Multiple Cartesian dispersed impacts (25 spheres): (a) deformation, (b) tension - component X.

The non-uniform state of residual stress is significantly influenced by the number of shots. Figure 11 shows that results converge with 13 impacts, but with 21 impacts the maximum residual stress is attained and the 25 shot model deteriorate the response. It indicates that the results are not improved with the increase of impacts.

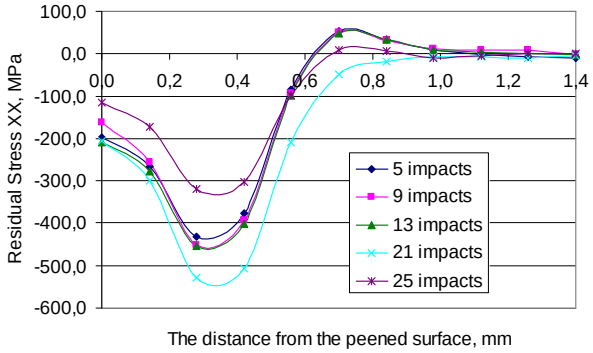

Figure 11. Residual stress - *XX* component profiles for various shot models at the center of the sample at a velocity of 36 m/s in multiple cartesian dispersed impact model.

- ***Radial Distribution***

Figure 12 shows the results of MSC.Dytran of strain and tension distribution after 25 impacts.

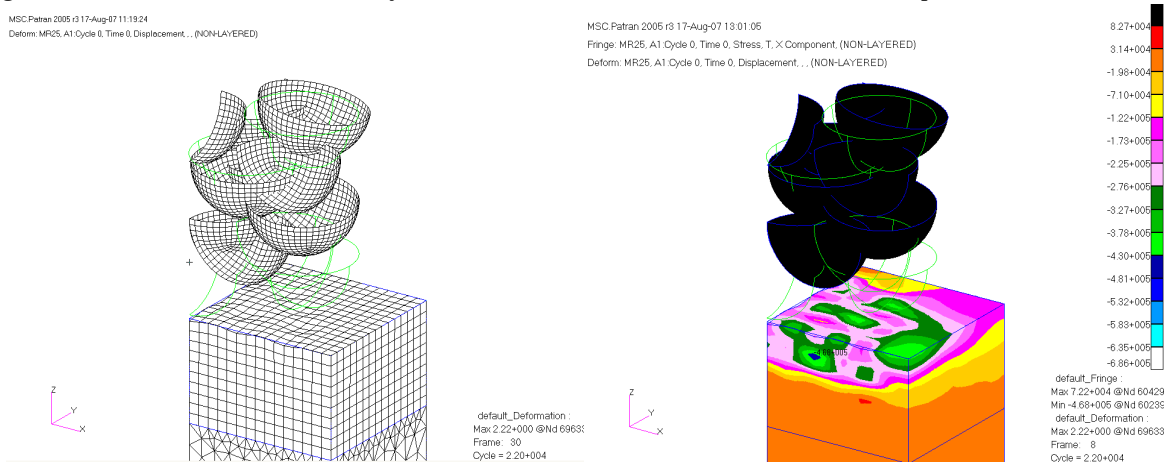

(a) (b)

Figure 12. Multiple Radial dispersed impact (25 spheres): (a) deformation, (b) stress - component *X*.

The non-uniform state of residual stress is significantly influenced by the number of shots. Figure 13 shows that the results in Radial model don't converge with 13 impacts, but with 21 impacts the maximum residual stress is attained again and the 25-shot model also deteriorate the response. It indicates that the results are not improved with closer impact model (Radial) but create instability.

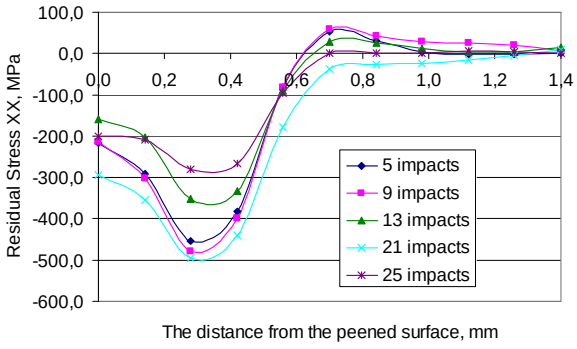

Figure 13. Residual stress - *XX* component profiles for various shot models at the center of the sample at a velocity of 36 m/s in multiple Radial dispersed impact model.

Comparing the residual stress profiles of 13 impacts in two points (A-middle of the block; B-middle of the symmetry) for the cartesian (Fig. 14a) and radial (Fig. 14b) models suggest that a uniform state of residual stress distribution in cartesian model is established, maintaining the Bielajev point and the depth of plastic zone (Fig. 15a).

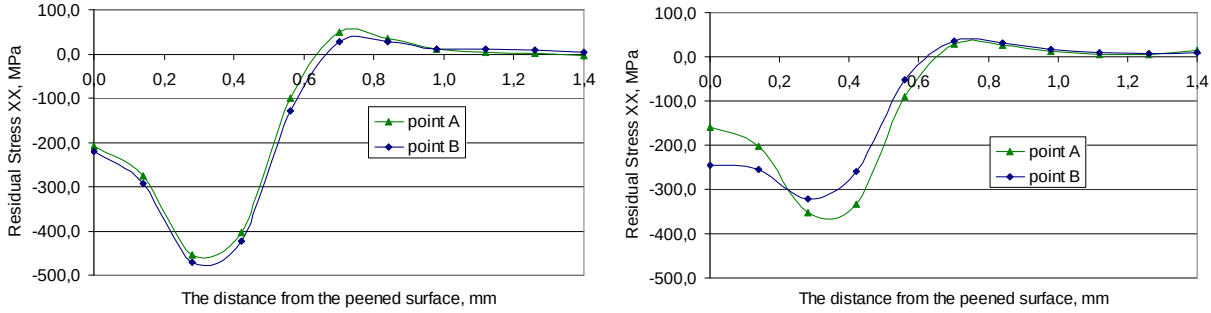

Figure 14. Residual stress - *XX* component profiles for 13-shot model at points A and B for dispersed impact model: (a) Cartesian and (b) Radial.

3.2. Static Modeling of Peen Forming

An implicit FE static analysis is done across the plate, which was blasted in the previous model to a reduced sample with explicit dynamic analysis. The FE mesh consists of only 300 shell elements with coarse elements of 5 x 5 mm^2 and thickness of the same number of layers and the same size of the solid sample. The restriction mentioned in section 2.2 is applied to the plate and the procedure of applying the residual stress as the initial condition of equivalent loading results in the deflection of the part as shown in Fig. 16 for an impact velocity of 36 m/s and 8 shots with the multiple concentrated impacts model when it reaches the saturation point.

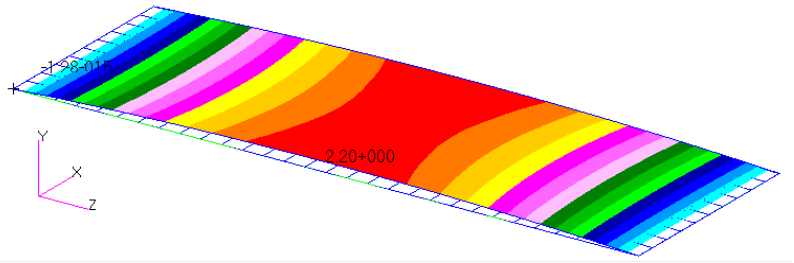

Figure 16. Deformed plate with the residual stress profile obtained with eight shots and v = 36 mm/s.

The 2.2 mm of deflection obtained in this work is validated by the result obtained by Han *et al.* (2002) of 2.1 mm for the same impact velocity after 32 steps of multiple impacts using a mesh of 4500 solid elements of 8 nodes, with a computational cost of 300 MB instead of only 50 MB with 300 shell elements of 4 nodes in this work (Silva, 2008).

4. CONCLUSION

The aim of this study was to determine the profile of mechanically induced residual stress resulting from shot peening metallic surfaces and the results of peen forming sheet blanks, both by numerical analysis using the finite element method for some proposed models validated by the literature.

A small-scale model of SP was adopted whereas the effect of ball impact is local; there is no need to blast the entire piece that can be very complex, and with an accuracy sufficient for a regular domain with the same material and subjected to the same blasting parameters; and finally, in those models it is only necessary to refine the mesh in the region of interest which is the region of impact.

The simple impact model represents the residual compressive stress profile, confirmed in this work, in which a stress peak occurs near the surface (Bielajev's point) as found in the literature.

The effect of speed and ball size on the profile of residual stress and deformation were evaluated. The influence is mainly on the thickness of the layer under compression, on the surface and subsurface stresses, and is very expressive on the deformation. The effect of material hardening is much smaller than these effects except on the surface stress. Friction converges to a value around 0.2, as mentioned by Han *et al.* (2000b), and significantly influences the surface stress profile and the Bielajev point. In addition, this work considered the effect of strain rate using the Cowper Symond

model. The results show the significant influence of strain rate on the compressed layer and on the Bielajev point, and that the deformation decreases significantly whereas the sensitivity to strain rate.

An alternative to the explicit dynamic simulation is still the very low cost model of equivalent loading, even though it is still difficult to specify the temperature, pressure or equivalent stress to obtain the workpiece final shape and the residual stress profile. There is a tendency to take the advantages of each model to define a hybrid model, since it is known that the explicit model is efficient in determining the plastic layer and the residual stress profile for the SP and the implicit solution is immediate to obtain the final form for PF.

Comparing the results of this work with MS.Dytran to other results with FEM codes like LUSAS (Barrios *et al.*, 2005), LS-DYNA (Bravo *et al.*, 2007), ABAQUS (Guagliano, 2001, Wang *et al.*, 2002), one could concluded that shot peening can be successfully simulated, but still with a prohibitive cost. It is still a challenge to compare simulation results with empirical results of measured residual stresses over the depth by expensive X-ray diffraction as done by Wang *et al.* (1998) for many materials of technological importance.

Further information about the work described here can be found in Silva (2008).

5. ACKNOWLEDGEMENTS

Authors acknowledge the financial support of CNPq and FINEP for this work.

6. REFERENCES

Al-Hassani, S.T.S., Kormi, K., Webb, D.C., 1999, “Numerical Simulation of Multiple Shot Peening”, The 7th International Conference o Shot Peening (ICSP - 7), pp. 217-227.

Barrios, D.B., Angelo, E., Gonçalves, E., 2005, “Finite Element Shot Peening Simulation for Residual Stress. Analysis and Comparison with Experimental Results”, VIII-MECON 2005, pp. 413-422, Argentina.

Bravo, C. M. A. C., Silva, E. C., Pavanello, R., Button, S.T., 2007, “Numerical Simulation of Forming Process Sheet Metal Blast Ball”, CMNE/CILAMCE 2007, pp. 217-227, Portugal.

Czekanski, A., Meguid, D.C., 2006, “On the use of variational inequalities to model impact problems of elasto-plastic media”, International Journal of Impact Engineering. pp. 1485-1511.

Guagliano, M., 2001, “Relating Almen instensity to residual stresses induced by shot peening: a numerical approach”, Journal of Materials Processing Technology, pp. 277-286.

Han, K., Peric, D., Crook, A.J.L., Owen, D.R.J., 2000a, “A combined finite/discrete element simulation of shot peening process. Part I: studies on 2D interaction laws”, Engineering Computations, v. 17, n. 5, pp. 593-619.

Han, K., Peric, D., Owen, D.R.J, Yu, J., 2000b, “A combined finite/discrete element simulation of shot peening process. Part II: 3D interaction laws”, Engineering Computations, v. 17, n. 6, pp. 680-702.

Han, K., Owen, D.R.J., Peric, D., 2002, “A combined finite/discrete element simulation of peen forming process”, Engineering Computations, v. 19, n. 1, pp. 92-118.

Levers, A., Prior, A., 1998, “Finite element analysis of shot peening”, Journal of Materials ProcessingTechnology. pp. 304-308.

Majzoobi,G.H., Azizi, R., Alavi Nia, A., 2005, “A three-dimensional simulation of shot peening process using multiple shot impacts”, Journal of Materials Processing Technology, 1226-1234.

Meguid, S. A., Shagal, G., Sranart, J. C., 1999a, “Finite element modeling of shot-peening residual stresses”. Journal of Materials Processing Technology. pp. 401-404.

Meguid, S. A. et al., 1999b, “Three-dimensional dynamic finite element analysis of shot-peening induced residual stresses”, Finite Element in Analysis and Design. v. 31, pp. 179-191.

Meguid, S. A. et al., 2002, “3D FE analysis of peening of strain-rate sensitive materials using multiple impingement model”, International Journal of Impact Engineering. v. 27, pp. 119-134.

MSC.Dytran 2005 r3, “Theory Manual, User Documentation: 2006”, MSC.Software Corporation.

Silva, E.C., Pavanello, R., Oliveira, R.S., Button, S.T., 2006, “Análise Numérica do Processo de Conformação de Chapas Metálicas por Jateamento de Esferas”, Proceedings of the XXVII CILAMCE - Iberian Latin American Congress on Computational Methods in Engineering, CD-ROM, pp. 1-15.

Silva, E.C., 2008, “Numerical Analysis of Shot Peen Forming of Metallic Sheets”, Doctoral Thesis, State University of Campinas, Campinas – SP, 242 pp.

Wang, S., Li, Yongjun, Y., Mei, W., 1998, “Compressive residual stress induced by shot peening forming”, Journal of Materials Processing Technology, pp. 64-73.

Wang, T., Platts, J., Levers, A., 2002, “Finite Element Impact Modeling for Shot Peen Forming”, Proceedings of the 8th International Conference on Shot Peening (ICSP-8), pp. 541-546.

7. RESPONSIBILITY NOTICE

The authors are the only responsible for the printed material included in this paper.